Journal of Optoelectronics and Advanced Materials Vol. 7, No. 5, October 2005, p. 2713 - 2720

# GRAIN SIZE EFFECTS IN METALLIC THIN FILMS PREPARED USING A NEW SPUTTERING TECHNOLOGY

M. Vopsaroiu*, M. J. Thwaites[a], G. V. Fernandez, S. Lepadatu, K. O'Grady

University of York, York, YO10 5DD, UK
[a]Plasma Quest Ltd., Hook, RG27 9UT, UK

In this paper we show how the grain size of metallic sputtered films can be controlled using a novel sputtering technology (HiTUS). This is evidenced by TEM and grain size analysis, which show changes of up to a factor 10 in the mean grain diameter of CoFe thin films. We achieved the grain size control by tuning the target bias voltage, which had the effect of changing the energy of the Ar ions. This is due to the unique design of the HiTUS sputtering plant in which the plasma generation is decoupled from the sputtering chamber and the bias voltage is not required to sustain a plasma glow discharge. Grain size control has been applied to a series of polycrystalline 20 nm thick CoFe films and a series of applications arising form the ability to control the grain size are presented. In particular, we show that the coercivity, resistivity and exchange bias field have a strong dependence on the mean grain size.

(Received July 6, 2005; accepted September 22, 2005)

*Keywords*: CoFe thin films, HiTUS plasma sputtering, Grain size control

## 1. Introduction

Thin film technologies are very important for applications in modern solid-state electronic devices, information storage, optical or protective coatings and various sensing devices. Most of these applications are based on polycrystalline thin films prepared using plasma sputtering, thermal evaporation or electro-deposition. As the thickness of the films is reduced to *nm* and *sub-nm* scales the properties of the films are dominated by their microstructure. One of the most important parameter of thin films is the final mean grain size and the ability to control the grain size is highly desirable for achieving specific properties. There are different methods for controlling the grain size or the texture including the use of additives [1,2], seed layers [3], post deposition annealing [4] or changes in the substrate temperature [5,6].

In this paper we present a novel plasma sputtering technology (HiTUS) that allows direct deposition of polycrystalline thin films with full control of the mean grain size. Details of the grain size control have been published previously [7]. TEM analysis is presented demonstrating the control of the grain size for CoFe thin films, followed by a presentation of some direct applications resulting from the grain size control. We are particularly interested in CoFe because of its high magnetic moment and low cost which makes it useful for applications such as soft underlayers in perpendicular media [8], core material of write elements in modern recording heads [9,10], ferromagnetic electrodes in spin tunnel junctions or MRAM devices [11]. However, depending on the specific application various properties of CoFe films (e.g. coercivity, saturation magnetization, electrical resistance or exchange coupling to an antiferromagnet) must be optimized. We achieved excellent control of these parameters by changing the grain size of films sputtered using HiTUS technology.

* Corresponding author: mv4@york.ac.uk

## 2. High target utilization sputtering (HiTUS) technology

Sputtering is generally the preferred option for coating technologies. Both conventional magnetron and ion beam sputtering have limitations regarding the deposition rate control. Magnetron sputtering in particular is also inefficient in terms of target utilization and does not allow sputtering from thick ferromagnetic targets. The sputtering technology described in this paper provides control of grain size, high uniform target utilization (> 90%) and the ability to sputter ferromagnetic materials efficiently with close control of deposition rates [12] (see also www.plasmaquest.co.uk). The system is based on a remotely generated high intensity plasma as shown in Fig. 1 and consists of a side arm launch tube as a plasma source linked to the main deposition chamber. The plasma is generated in the side arm by an RF electric field (max. 2.5 kW). Energy is transferred to the plasma by electrons via the mechanism of Landau damping. The plasma is then launched into the chamber via the interaction of the RF field with the launch electromagnet and then steered onto the target by a second electromagnet.

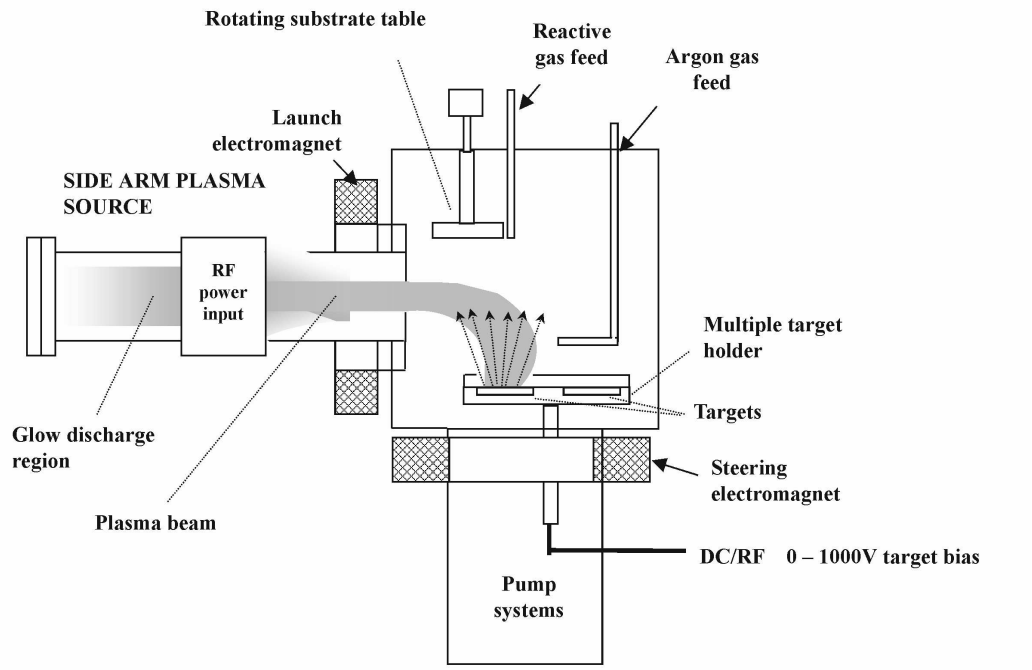


Fig. 1. Schematic representation of a HiTUS sputtering plant.

Experiments have shown that the typical electron energy in the HiTUS System, under our standard working conditions (Ar process pressure of $3 \times 10^{-3}$ mbar, RF power of 2 kW) is of the order of 65 eV and energies in excess of this figure are readily obtainable. It is known that electrons with energies in excess of 15.76 eV are required in order to ionize Ar neutrals. Hence this technology offers highly efficient ionisation, which was also confirmed by optical emission spectroscopy. The spectra in Fig. 2 show the increase in plasma ionization of the HiTUS system (density ~ $10^{12}$ – $10^{13}$ ions $cm^{-3}$) compared with that achieved in a conventional magnetron plasma (density ~ $10^{10}$ ions $cm^{-3}$).

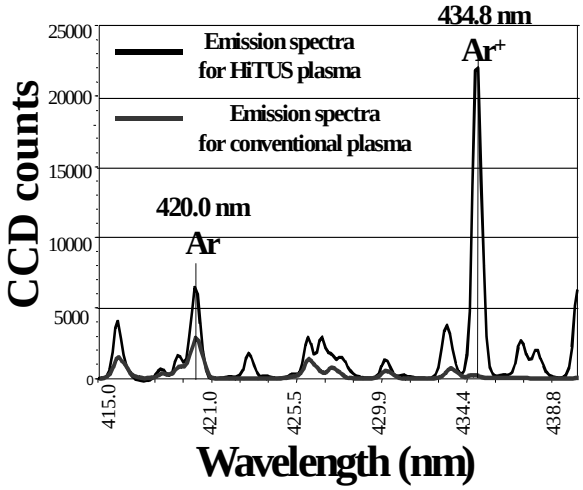


Fig. 2. Comparison of optical emission spectrum of high density plasma (~ $10^{13}$ ions $cm^{-3}$) and conventional plasma (~ $10^{10}$ ions $cm^{-3}$). The strong emission peak at 434.8 nm corresponds to $Ar^+$.

The coupled magnetic flux lines of the launch and steering electromagnets confine the plasma electrons. By altering the current applied to the electromagnets and in particular to the steering electromagnet, the magnetic field strength is altered and the coupling of the flux lines of the electromagnets alters slightly. The position of the plasma beam can therefore be adjusted to ensure good beam coverage of the target surface. A negative DC bias (–1 V to - 1000 V) can be applied to the target, although in HiTUS technology a bias voltage is not required to sustain a plasma glow discharge. The application of the negative DC bias results in the positively charged $Ar^+$ ions being accelerated across the target sheath leading to sputtering of the material.

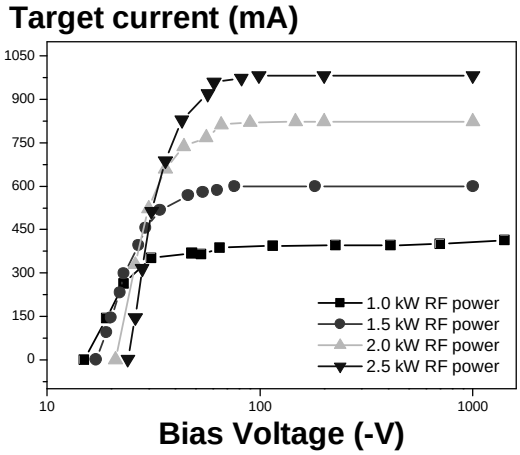


Fig. 3. Target current versus bias voltage for different RF power showing the saturation of the target current at bias voltages just over 100 V.

Sputtering from dielectric targets can be achieved using an RF bias. Above approximately 100 V bias the target current saturates and is independent of voltage as shown in Fig. 3. This enables deposition rates to be varied whilst maintaining a high-density plasma.

A very important characteristic of HiTUS is its ability to sputter from ferromagnetic materials without the use of magnetic fields beneath the target. This allows sputtering from thick ferromagnetic targets, which is a major limitation in conventional magnetron sputtering systems and is of particular interest in the magnetic recording industry. In this paper we focus on the ability of HiTUS to sputter thin films with controlled grain size and the potential applications arising from this.

## 3. Sputtering of thin films with controlled grain size

In our previous work we reported that the grain size of HiTUS sputtered films is only controlled via the growth rate [7], which could be varied by changing RF power, bias voltage or the Ar process pressure [13]. However, based on our recent work on CoFe films it appears that the grain size is primarily controlled by the bias voltage, which in turn controls the energy of atoms in the growing film. A higher bias increases the energy of the ions generating enhanced surface diffusion that results in the larger grains growth. These results are supported by detailed TEM and grain size analysis.

Six 20 nm thick CoFe samples were sputtered directly onto Si substrates without using seed layers. A magnetic field of 100 Oe was applied during deposition to induce a uniaxial magnetic anisotropy. All films were sputtered after pumping to a base pressure of $3 \times 10^{-7}$ mbar with Ar process pressure of $2.7 \times 10^{-3}$ mbar. The RF power used to generate the plasma in the HiTUS system was kept constant at 1.75 kW. Prior to each deposition, the target and substrate were plasma cleaned to eliminate contamination or oxide layers. Substrate heating was not employed and during sputtering the substrate temperature lay in the range of 30 – 70 $^0$C.

Table 1. Growth conditions and sample specifications.

| Sample | Bias Voltage (- V) | Growth rate (Å/s) | Mean grain size D (nm) | Coercivity $H_c$ (Oe) |
|---|---|---|---|---|
| **A** | 120 | 0.1 | 7.2 | 9 |
| **B** | 200 | 0.2 | 22 | 20 |
| **C** | 400 | 0.4 | 49 | 120 |
| **D** | 600 | 0.5 | 52 | 126 |
| **E** | 800 | 0.7 | 60 | 123 |
| **F** | 1000 | 0.8 | 79 | 121 |

In order to change the grain size, the DC bias voltage was varied systematically (Table 1). The thickness of the films was kept constant at 20 nm while the sputtering rate ranged between 0.1 to 0.8 Å/s (Table 1).

Sample A - 120 V bias

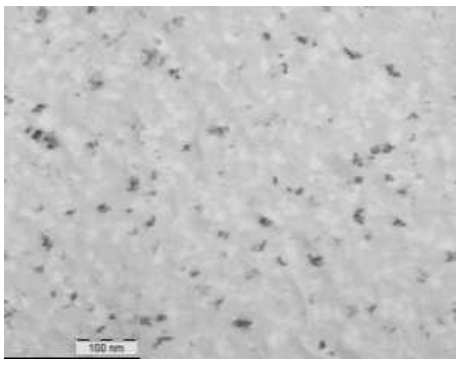


Fig. 4. TEM image of sample A sputtered at 120 V bias resulting in ≈ 7 nm grain size.

Sample F - 1000 V bias

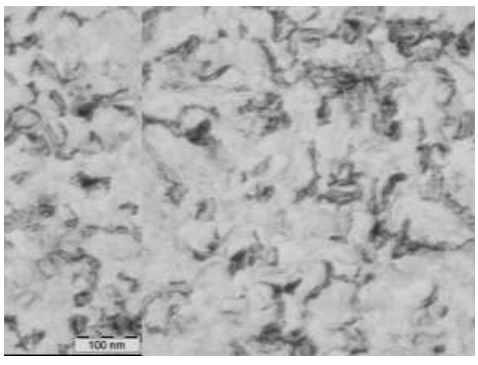


Fig. 5. TEM image of sample F sputtered at 1000 V bias resulting in ≈ 80 nm grain size.

Grain size measurements were performed using TEM imaging of grids that were attached to each substrate. TEM images were acquired for each sample in bright field mode at 120 kV and x150 k magnification. The mean grain size was obtained by measuring and counting over 500 particles for each sample using a Zeiss particle size analyser. Typical TEM images for two extreme samples A and F are shown in Figs. 4 and 5. The crystal structure was determined using X-ray diffraction and was found to be BCC with a dominant (110) crystallographic orientation.

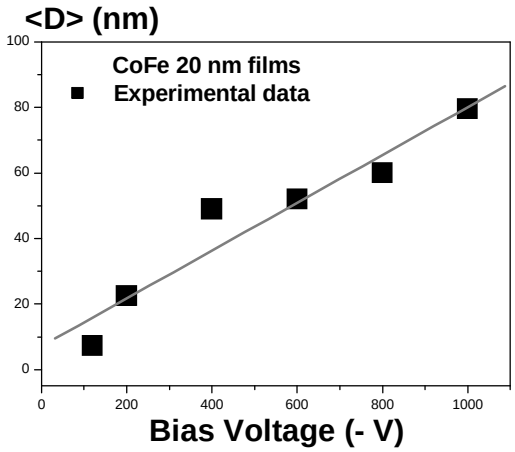


Fig. 6. Grain size variation as a function of the bias voltage.

Mean grain diameters as small as 7.2 nm have been achieved at 120 V bias generating a sputtering rate of 0.1 Å/s. For a bias of 1000 V the sputtering rate was 0.8 Å/s and a mean grain size of 80 nm resulted. Fig. 6 shows the change in the mean grain size as a function of the bias voltage for all samples. The six CoFe samples have been measured to determine the effect of the grain size on magnetic and electric properties.

## 4. Effect of grain size on the coercivity

Fig. 7 shows the normalised hysteresis loop for each CoFe sample measured with a VSM at room temperature in the easy axis direction. Although the loops have similar squareness with sharp magnetization reversal, there is a clear difference between the coercivity of the samples having the smallest mean grain size A and B and those with larger mean grain size (C to F).

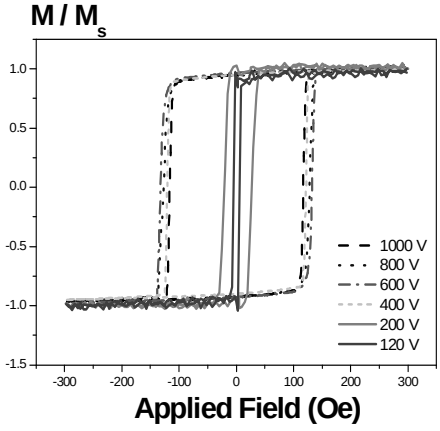


Fig. 7. Room temperature hysteresis loops of CoFe samples A – F.

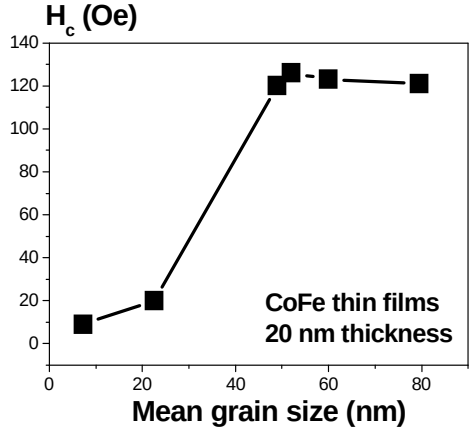


Fig. 8. Coercivity variation versus mean grain size.

CoFe thin films exhibit naturally large coercivities and soft magnetic properties are usually achieved using seed layers [14]. In the present study we obtained a reduction of coercivity of CoFe films from around 120 Oe down to 9 Oe due to a reduction in the mean grain size. Fig. 8 shows the coercivity as a function of the mean grain size. Samples with mean grain diameter below 30 nm show soft magnetic properties with coercivities of less than 25 Oe and a minimum of 9 Oe. As the mean grain size increases there is a sharp increase in the coercivity up to around 120 Oe for grain sizes larger than 50 nm, which remains almost constant for grain sizes in the range 50 to 100 nm. The coercivity variation with the grain size in polycrystalline ferromagnetic films is well described by the random anisotropy model [15, 16], which is in good agreement with our results. For grain size below the exchange length ( $L_{ex} = \sqrt{A/K_u}$ ) the model predicts a coercivity dependence of the grain size as ~ $D^6$ (or ~ $D^3$ when the thickness of the film is considered, as in our case). For an exchange constant $A \approx 5.8 \times 10^{-8}$ erg/cm and anisotropy constant $K_u \approx 2.7 \times 10^5$ erg/cm$^3$ we obtained $L_{ex} \approx 46$ nm for our samples. This value is in good agreement with the mean grain size below which a significant reduction in coercivity is observed (see Fig. 8). According to the model, the coercivity is then constant as long as the mean grain size is smaller than the domain wall width (δ), which for a BCC structure is given by $\delta = \frac{\pi}{\sqrt{2}} L_{ex}$. We calculated that δ ≈ 100 nm for our samples, which is larger than the largest man grain size, and the plateau region in Fig. 8 is observed.

## 5. Effect of grain size on the resistivity

It is well known that the electrical resistivity of polycrystalline thin films can vary substantially in comparison to that of bulk [17]. For metallic thin films of constant thickness the electrical resistivity can be varied a few orders of magnitude by changing the grain size of the films. Changes of about a factor 10 have been found in room temperature electrical measurements of our CoFe films shown in Fig. 9, where the electrical resistivity is plotted as a function of the mean grain size.

Films with small grain size show high resistivity while for the larger grained samples the resistivity decreases exponentially approaching the bulk value. This can be explained in terms of scattering at the grain boundaries in addition to the bulk scattering centres.

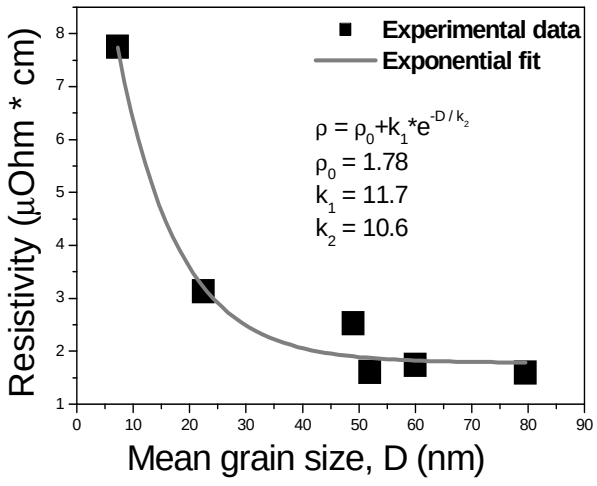


Fig. 9. Electrical resistivity as a function of the mean grain size for CoFe 20 nm thin films.

Electric carriers moving through a thin film containing small grains would suffer extra scattering at the grain boundaries and therefore they have a reduced mean free path. Tuning the electrical properties of the thin films via the grain size is very important for applications where different properties are required for thin film electrodes or resistors.

## 6. Effect of grain size on the exchange bias field

The exchange bias effect is a shift in the hysteresis loop of a ferromagnet (FM) when it is in contact with an anti-ferromagnet (AFM) [18]. This effect is widely used to pin the magnetisation direction of a hard layer in a GMR spin valve or TMR sensor [19]. Achieving a large exchange bias field is required to improve the efficiency of the pinning. It is known that the room temperature exchange bias effect is affected by thermal activation within the AFM [20], interface properties [21], thickness of FM [5] and AFM layers [22], structure of the seed layers [23] and the grain size of the AFM layer [24]. We have used CoFe films as the FM layer in a set of exchange bias samples with the structure Si/CoFe(5 nm)/IrMn(6 nm)/Ta(10 nm), in order to observe the effect of the grain size of CoFe on the exchange bias field. CoFe layers were deposited in exactly the same conditions as the CoFe samples A to F except that the thickness of the layers was reduced to maximize the exchange pinning.

As the CoFe layers were prepared under different bias conditions, a change in the mean grain size is expected. However, we have no direct grain size analysis for this set of samples and the exchange bias field will be represented in terms of the bias voltage rather than the grain size.

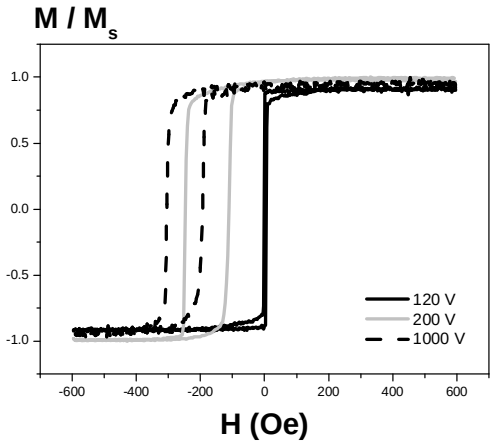


Fig. 10. Examples of exchanged bias hysteresis loops for CoFe/IrMn bilayers. CoFe sputtered under different bias.

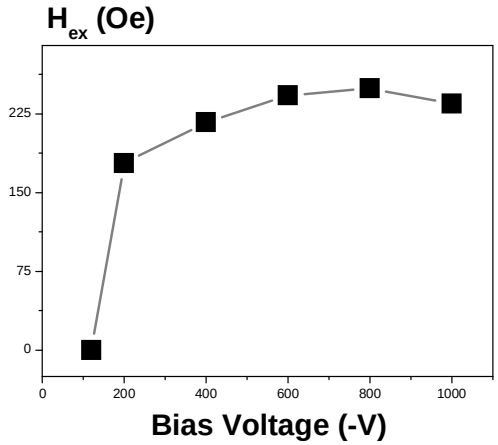


Fig. 11. Exchange bias field variation with the CoFe bias voltage.

IrMn layers were sputtered under identical conditions using $3 \times 10^{-7}$ mbar base pressure, $2.75 \times 10^{-3}$ mbar Ar process pressure, 2.00 kW RF Power and – 300 V DC bias voltage. All samples were measured at room temperature using a VSM. The loops show an increasing shift towards negative field values due to the exchange bias field (Fig. 10). The effect of the bias voltage (e.g. CoFe grain size) on the exchange bias field is plotted in Fig. 11. The data clearly indicates that enhanced exchange bias can be achieved by increasing the grain size of the FM layers. For the CoFe films sputtered at 120 V bias voltage there is no exchange bias indicating that probably the field generated by the small CoFe grains was not large enough to induce the parallel coupling at the AFM/FM interface. For CoFe films sputtered at bias voltages > 200 V the films contain larger grains and the coupling to the AFM is sufficient to induce the shift in the hysteresis loops. This also appears to saturate for bias voltages larger than 300 V, which should correspond to grains larger than 25 nm.

## 7. Conclusions

We have presented a novel sputtering technology (HiTUS) that offers a number of potential advantages over currently available deposition techniques. In particular, we have demonstrated the ability of HiTUS to control the grain size of CoFe sputtered thin films. We have shown that grain size can be controlled via the target bias voltage. Changing the bias voltage has the effect of changing the Ar ion energy and therefore the energy of the atoms that results in the growth of the grains. Achieving different growth conditions is a unique feature of HiTUS due to the separation of the plasma generation from the deposition chamber.

A series of CoFe films with different grain size has been prepared. Magnetic and electric properties of the CoFe films have been determined and the results correlated to the changes in the grain size. We showed that films with small grain size exhibit soft magnetic properties, high resistivities and no exchange bias when grown in contact with an antiferromagnet. At the other extreme when the grain size is large, the films have large coercivities, close to bulk resistivities and large exchange bias. Therefore, thin film properties can be tuned to specific needs by changing the grain size.

**Acknowledgements**

The authors would like to acknowledge that this project was financially supported by the UK Department of Trade and Industry, LINK ISD Programme and the EU Research Training Network "NEXBIAS".

## References

[1] N. Tani, T. Takahashi, M. Hashimoto, M. Ishikawa, Y. Ota, K. Nakamura, IEEE Trans. Magn., **27**, 4736 (1991).
[2] A. Ajan, I. Okamoto, J. Appl. Phys. **92**, 6099 (2002).
[3] L. L. Lee, D. E. Laughlin, D. N. Lambert, IEEE Trans. Magn. **30**, 3951 (1994).
[4] R. B. Kale, C. D. Lokhande, Appl. Surface Sci. **223**, 343 (2004).
[5] J. A. Thornton, J. Vac. Sci. Technol. **11**, 666 (1974).
[6] I. Petrov, P. B. Barna, L. Hultman, J. E. Greene, J. Vac. Sci. Technol. A, **21**, S117 (2003).
[7] M. Vopsaroiu, G. V Fernandez, M. J. Thwaites, J. Anguita, P. J. Grundy, K. O'Grady, J. Phys. D: Appl. Phys. **38**, 490-496 (2005).
[8] D. Litvinov, M. K. Kryder, S. Khizroev, J. Magn. Mag. Mat. **232**, 84 (2001).
[9] Tetsuya Osaka, Electr. Acta **44**, 3885 (1999).
[10] F. Lallemand, D. Comte, L. Ricq, P. Renaux, J. Pagetti, C. Dieppedale, P. Gaud, Appl. Surf. Science **225**, 59 (2004).
[11] S. Cardoso, C. Cavaco, R. Ferreira, L. Pereira, M. Rickart, P. P. Freitas, N. Franco, J. Gouveia, N. P. Barradas, J. Appl. Phys. **97**, 10C916 (2005).
[12] M. J. Thwaites, "High density plasmas" USA Patent No. 6463873, 15 Oct. 2002.
[13] M. Vopsaroiu, M. J. Thwaites, S. Rand, P. J. Grundy, K. O'Grady, IEEE Trans. Magn. **40**, 2443 (2004).
[14] H. S. Jung, W. D. Doyle, S. Matsunuma, J. Appl. Phys. **93**, 6462 (2003).
[15] R. Alben, J. J. Becker, M. C. Chi, J. Appl. Phys. **49**, 1653 (1978).
[16] G. Herzer, IEEE Trans. Magn. **26**, 1397 (1990).
[17] K. L. Chopra, Thin Film Phenomena, (1969).
[18] W. H. Meiklejohn, C. P. Bean, Phys. Rev. **102**, 1413 (1956).
[19] J. R. Childress, M. J. Carey, R. J. Wilson, N. Smith, C. Tsang, M. K. Ho, K. Carey, S. A. MacDonald, L. M. Ingall, B. A. Gurney, IEEE Trans. Magn. **37**, 1745 (2001).
[20] L. E. Fernandez-Outon, K. O'Grady, M. J. Carey, J. Appl. Phys. **95**, 6852 (2004).
[21] A. M. Choukh, IEEE Trans. Magn. **33**, 3676 (1997).
[22] M. Tsunoda, M. Konoto, K. Uneyama, M. Takahashi, IEEE Trans. Magn. **33**, 3688 (1997).
[23] H. Sang, Y. W. Du, C. L. Chien, J. Appl. Phys. **85**, 4931 (1999).
[24] M. Pakala, Y. Huai, G. Anderson, L. Miloslavsky, J. Appl. Phys. **87**, 6653 (2000).
[25] S. Manzoor, M. Vopsaroiu, G. Vallejo-Fernandez, K. O'Grady, J. Appl. Phys. **97**, 10K118 (2005).